UCSF
UC San Francisco Previously Published Works

Title

Stromally Derived Lysyl Oxidase Promotes Metastasis of Transforming Growth Factor-β–Deficient Mouse Mammary Carcinomas

Permalink

https://escholarship.org/uc/item/4qp3x5r2

Journal

Cancer Research, 73(17)

ISSN

0008-5472

Authors

Pickup, Michael W
Laklai, Hanane
Acerbi, Irene
et al.

Publication Date

2013-09-01

DOI

10.1158/0008-5472.can-13-0012

Peer reviewed

eScholarship.org Powered by the California Digital Library
University of California

NIH Public Access
Author Manuscript
Cancer Res. Author manuscript; available in PMC 2014 September 01.

Published in final edited form as:
Cancer Res. 2013 September 1; 73(17): 5336–5346. doi:10.1158/0008-5472.CAN-13-0012.

Stromally Derived Lysyl Oxidase Promotes Metastasis of Transforming Growth Factor-β Deficient Mouse Mammary Carcinomas

Michael W. Pickup[1], **Hanane Laklai**[2], **Irene Acerbi**[2], **Philip Owens**[1], **Agnieszka E. Gorska**[1], **Anna Chytil**[1], **Mary Aakre**[1], **Valerie M. Weaver**[2], and **Harold L. Moses**[1]

[1]Department of Cancer Biology, Vanderbilt University School of Medicine and Vanderbilt-Ingram Cancer Center, 698 Preston Research Building, 2220 Pierce Ave., Nashville, TN 37212

[2]Department of Surgery and Center for Bioengineering and Tissue Regeneration, University of California at San Francisco, Department of Surgery, 513 Parnassus Ave, HSE 565, San Francisco, CA 94143-0456

Abstract

The tumor stromal environment can dictate many aspects of tumor progression. A complete understanding of factors driving stromal activation and their role in tumor metastasis is critical to furthering research with the goal of therapeutic intervention. Polyoma middle T-induced mammary carcinomas lacking the type II TGF-ß receptor ($PyMT^{mgko}$) are highly metastatic compared to control PyMT-induced carcinomas ($PyMT^{fl/fl}$). We hypothesized that the $PyMT^{mgko}$ activated stroma interacts with carcinoma cells to promote invasion and metastasis. We show that the extracellular matrix associated with $PyMT^{mgko}$ tumors is stiffer, has more fibrillar collagen, and increased expression of the collagen crosslinking enzyme lysyl oxidase (LOX) compared to $PyMT^{fl/fl}$ mammary carcinomas. Inhibition of LOX activity in $PyMT^{mgko}$ mice had no effect on tumor latency and size, but significantly decreased tumor metastasis through inhibition of tumor cell intravasation. This phenotype was associated with a decrease in keratin 14 positive myoepithelial cells in $PyMT^{mgko}$ tumors following LOX inhibition as well as a decrease in focal adhesion formation. Interestingly, the primary source of LOX was found to be activated fibroblasts. LOX expression in these fibroblasts can be driven by myeloid cell-derived TGF-ß, which is significantly linked to human breast cancer. Overall, stromal expansion in $PyMT^{mgko}$ tumors is likely caused through the modulation of immune cell infiltrates to promote fibroblast activation. This feeds back to the epithelium to promote metastasis by modulating phenotypic characteristics of basal cells. Our data indicate that epithelial induction of microenvironmental changes can play a significant role in tumorigenesis and attenuating these changes can inhibit metastasis.

Keywords

LOX; Collagen; Fibroblast; TGF-β; Metastasis

Introduction

The stromal microenvironment of a tumor is an essential component of tumor progression(1). Comprised of various resident and recruited cell types as well as extracellular proteins, the stromal components can determine phenotypic characteristics and

Conflicts of Interest: No conflicts of interest to report.

NIH-PA Author Manuscript
NIH-PA Author Manuscript
NIH-PA Author Manuscript

NIH-PA Author Manuscript

NIH-PA Author Manuscript

NIH-PA Author Manuscript

ultimately patient outcome. By providing growth factors and other migratory signals as well as depositing scaffolding proteins, the tumor stroma can effectively drive or impede a tumor cell toward intravasation and metastatic colonization(2). Specifically, matrix deposition and remodeling, largely facilitated through fibroblast mediators, promotes tumor growth and migration(3). While stromal influence is acknowledged, a full understanding of the signals driving the formation of a tumor promoting stroma as well as the reciprocal response of the epithelium to these changes has yet to be obtained. Insights into these interactions will provide the backbone for future therapeutic interventions specifically targeting tumor-stromal crosstalk.

Extracellular matrix (ECM) proteins, and in particular collagen, are a major component of the tumor microenvironment and exert significant effects on the tumor epithelium(4). Through its integrin mediators, extracellular matrix proteins encourage tumor growth and invasiveness. Increased mammographic density, which is significantly associated with collagen levels, independently predicts increased probability of occurrence of breast cancer in patients(5). These results are mimicked in murine models of breast cancer progression in which deposition of collagen that is unable to be proteolytically cleaved results in increased tumor formation as well as increased lung metastasis(6). Recently, it has been appreciated that ECM-epithelial crosstalk is not only mediated by the ECM proteins themselves, but by the orientation and crosslinking status of the collagen fibers. Lysyl Oxidase (LOX) is a matrix modifying enzyme that cross-links and stiffens collagen fibers to promote their stability(3). LOX has garnered interest in breast cancer as an important enzyme regulating stromal modification to drive malignant progression(3). Although epithelial LOX has been implicated in tumor metastasis through the promotion of a TGF-β driven Epithelial to Mesenchymal Transition (EMT) and integrin mediated epithelial invasion(7), the role of stromal LOX in tumor metastasis has yet to be examined.

Previous work from our laboratory showed that abrogation of TGF-β signaling in epithelia results in a significant increase in PyMT driven mammary carcinoma metastasis(8). Looking at the primary tumor for a potential cause of this phenotype, one of the most striking observations was an expansion of the stromal microenvironment (9). As these tumors presented with increased levels of TGF-β derived from infiltrated myeloid derived suppressor cells and an increase in αSMA positive fibroblasts, we hypothesize that these activated fibroblasts are driving stromal expansion through the increased expression of LOX. The current study aimed to identify differentially regulated matrix associated genes resulting in increased stromal expansion in the $PyMT^{mgko}$ model of breast cancer and to examine their role in driving epithelial cell phenotypes which ultimately results in metastasis. To address this question, we used our established $PyMT^{mgko}$ model of mammary tumor progression. The findings show that TGF-ß secreted by myeloid cells induces expression of LOX by carcinoma-associated fibroblasts, which in turn increases matrix crosslinking and stiffness to drive Keratin 14 cell FAK signaling, carcinoma cell intravasation and metastasis.

Methods

Mouse Model

TβRII(fl/fl) mice were crossed with MMTV-PyVmT/MMTV-Cre/TβRII(fl/fl) transgenic mice to produce the TβRII(fl/fl)/PyMT ($PyMT^{fl/fl}$) and TβRII(fl/fl)/PyMT/MMTV-Cre ($PyMT^{mgko}$)mice. Cell lines were isolated from these spontaneous tumors and used in further *in vitro* experimentation. LOX inhibition studies used Beta-Aminopropriontrile (3mg/ml, Sigma) dissolved in the drinking water. Mice were housed and handled according to approved Institutional Animal Care and Use Committee protocols.

NIH-PA Author Manuscript

NIH-PA Author Manuscript

NIH-PA Author Manuscript

Lung Whole Mount and Circulating Tumor Cell analysis

Lungs were fixed in 10% neutral buffered formalin overnight at 4°C. The next day, lungs were dehydrated, placed in xylene for 1 h, and then changed to fresh xylene overnight. Lungs were rehydrated before dipping in Mayer's hematoxylin for 2 min and then washed in running tap water for 5 min. Tissues were destained in HCl (fresh 1% v/v from a 12 N solution) for 20 min, rinsed in running tap water overnight, dehydrated, and placed in xylene overnight before counting of stained metastatic tumor foci under a dissecting light microscope.

Circulating blood was isolated from the left ventricle of tumor bearing mice upon sacrifice. 200uL of the blood was plated into a well of a gelatin coated 6 well dish and allowed to grow for 3 to 4 weeks. After the growth phase, colonies larger than 150um were counted and quantified.

Picrosirius Red Staining and Quantification

Five μm5 micron sections of paraffin-embedded mammary tumors were stained with 0.1% Picrosirius Red (Direct Red 80; Sigma Aldrich). Stained sections were imaged on a Zeiss Axiophot equipped with a cross-polarizer. Images were quantified for pixel density of thresholded light intensity(3).

In situ hybridization

The following protocol was performed on sections of fresh frozen tumor tissue. In brief, sections were digested with 0.125mg/ml of pronase, fixed in 10% formalin and blocked with 0.2% glycine. Sections were probed with Digoxigenin labeled sense and anti-sense probes, each ~300bp in length. Probes were obtained from digestion of full length mouse LOX cDNA with HindIII and XbaI (New England Biolabs). Following overnight probe incubation, staining was visualized through staining sections with 1:500 AP-labeled anti-DIG (Roche). Sections were counterstained with DAPI (Invitrogen) for nuclei visualization(10).

Tissue preparation for AFM measurements of ECM stiffness

Mammary glands were analyzed following cryopreservation. Fresh glands were embedded in OCT (Tissue-Tek) aqueous embedding compound within a disposable plastic base mold (Fisher) and were snap frozen by direct immersion into liquid nitrogen. Frozen tissue blocks were then cut into 20 μm sections using disposable low profile microtome blades (Leica, 819) on a cryostat (Leica, CM1900-3-1). Prior to the AFM measurement, each section was thawed by immersion in PBS at room temperature. The samples were maintained in proteinase inhibitor in PBS (PROTEASE INHIBITOR COCKTAIL Roche Diagnostics, 11836170001), with Propidium Iodide (SIGMA P4170, 20 μg/ml) during the AFM session.

Two-photon microscopy image acquisition and analysis

For two-photon imaging, we used custom resonant-scanning instruments based on published designs containing a five-PMT array (Hamamatsu, C7950) operating at video rate(11). The setup was used with two channel simultaneous video rate acquisition via two PMT detectors and an excitation laser (2W MaiTai Ti-Sapphire laser, 710-920nm excitation range). Second harmonics imaging was performed on a Prairie Technology Ultima System attached to an Olympus BX- 51 fixed stage microscope equipped with a 25× (NA 1.05) water immersion objective. Unfixed, hydrated samples were exposed to polarized laser light at a wavelength of 830nm and emitted light was separated with a filter set (short pass filter, 720nm; dichroic mirror, 495nm; band pass filter, 475/40nm). Images of x-y planes of 284 by 284μm at a resolution of 0.656μm/pixel were captured using Micro-Manager Open Source Microscopy

NIH-PA Author Manuscript

NIH-PA Author Manuscript

NIH-PA Author Manuscript

Software (Micro-Manager) in at least 3 locations on each mammary gland. Quantification of collagen fibers was achieved by setting a minimal threshold in the second harmonic signal. The threshold was maintained for all images across all conditions. The area of regions that was covered by the minimal threshold was calculated and 3 images per sample were averaged together (Image J, Image Processing and Analysis in Java). Collagen fiber diameters data were visualized and analyzed using Imaris (Bitplane AG) and MATLAB (MathWorks).

Statistics

Statistical analysis was performed using Graphpad Prism after consultation with the Vanderbilt Biostatistics Department.

Results

Increased Collagen Deposition and LOX Expression in PyMT^{mgko} Tumors

The generation of mammary tumors with and without TGF-β Type II receptor has been previously described(8, 9). Prior work showed this mouse model presents with an enhanced reactive stroma and increased myofibroblast presence compared to tumors with TGF-β signaling(9). Expanding on these studies, characterization of the collagenous extracellular matrix was performed. Elevated Trichrome Blue staining and increased polarized intensity of Picrosirius Red stained tissue suggested higher content of total and fibrillar collagen in the stroma of PyMT^{mgko} tumors(Figure 1A and B). Q-PCR analysis indicated no increased expression of Collagen Type I or Type 4 implicating collagen stablization (Supplemental Figure 1). Second harmonics generation revealed a trend of more abundant linearized, thick collagen fibers dispersed throughout the stroma, consistent with a greater amount of cross-linked collagen present in the PyMT^{mgko} tumors, presented and quantified in Figure 1C. Consistently, tumor gene expression and protein levels showed that expression of the collagen crosslinking enzyme LOX was increased in the PyMT^{mgko} tumors compared to PyMT$^{fl/fl}$ tumors (Figure 1D). This protein specifically cross-links collagen fibers to regulate their stability(12). LOX was of particular interest due to its significant role in tumor progression(13). Analysis of other members of the LOX family showed no significant difference between PyMT$^{fl/fl}$ and PyMT^{mgko} tumors (supplemental figure 2). Concordant with increased expression of LOX, atomic force microscopy indentation quantified a significant increase in the stiffness of the extracellular matrix associated with the PyMT^{mgko} tumors (Figure 1E). These results indicate that rather than enhanced collagen synthesis, PyMT^{mgko} tumors promote increased collagen stability culminating in an overall increase in collagen deposition and stiffness in the stroma associated with PyMT^{mgko} tumors.

LOX Inhibition Prevents Tumor Cell Metastasis Through Decreased Tumor Cell Extravasation

TGF-β has long been known to promote metastasis in late stage tumors through the induction of an EMT, however epithelial loss of TGF-β signaling in our mammary tumors presents with increased metastatic burden(8). As LOX expression was significantly increased in PyMT^{mgko} tumors, the effect of this increased expression on the enhanced lung metastasis of the PyMT^{mgko} tumors was examined. Beta-Aminoproprionitrile (BAPN), a synthetic chemical inhibitor of LOX activity that mimics the efficacy of LOX inhibitory antibodies and was used in our mouse model(13-15). Treatment of PyMT^{mgko} mice with BAPN resulted in no significant change in time to tumor palpation (Figure 2A). Atomic force microscopy indentation mapping performed on those tumors treated with and without BAPN showed a significant reduction in the tensile strength of the stromal regions of these tissues (Figure 2B). Histological analysis of the primary tumor showed no changes to the composition or characteristics of the tumor epithelium or stromal infiltrates (Figure 2C).

NIH-PA Author Manuscript

NIH-PA Author Manuscript

NIH-PA Author Manuscript

BAPN treatment also did not cause any significant changes in tumor volume in PyMT^{mgko} mice (Figure 2D). However, upon examination of lung whole mounts from PyMT^{mgko} mice with and without BAPN treatment, there was a significant decrease in the incidence of lung metastasis following BAPN treatment (Figure 2E). Additionally, in those PyMT^{mgko} mice that did harbor lung metastasis upon BAPN treatment, the number of lung metastasis was significantly lower than in the untreated PyMT^{mgko} mice (Figure 2F). In the cascade of metastatic progression, intravasation from the primary tumor into the vasculature is one of the first steps(16). Upon examination, we noted a reduced numbers of viable tumor cells in the circulation suggesting that LOX inhibition significantly reduced metastasis by inhibiting tumor cell intravasation (Figure 2G). As premetastatic niche effects of LOX have been established(17), tail vein injection experiments into mice with and without BAPN treatment were performed and showed no differences in metastatic colonization potential (Supplemental Figure 3). Thus, these data suggest that LOX promotes tumor cell metastasis in PyMT^{mgko} tumors by enhancing intravasatation into the vasculature.

LOX Promotes Keratin 14 Myoepithelial Cells

Since we showed that LOX promoted tumor cell escape from the primary tumor into the vasculature, we next looked for correlations between LOX and phenotypic molecular changes associated with highly aggressive, metastatic tumors. Gene expression analysis revealed that LOX inhibition in PyMT^{mgko} tumors decreased the expression of keratin 14 (Figure 3A). These findings were supported by immunofluorescence which demonstrated that PyMT^{mgko} tumors were highly enriched for K14 cells, particularly at the epithelial stromal interface implicating a role for collagen interaction in this phenotype. Indeed, BAPN-treated tumors showed a significant reduction in K14+ epithelial cells (Figure 3B, Supplemental Figure 4). These findings are consistent with the basal subtype of breast cancer which presents with increased metastasis and poor patient survival(18). As myoepithelial cells represent a highly contractile, matrix responsive cell population and previous studies indicated that LOX-mediated collagen cross-linking and stiffening promote the formation of focal adhesions(3, 19, 20), we addressed the relationship between these two phenotypes. Upon treatment with BAPN, levels of pFAK-397 relative to total FAK were decreased in total tumor lysates (Figure 3C). Immunoflourence of PyMT^{mgko} tumors either untreated or treated with BAPN stained for Keratin 14 and pFAK showed that decreased pFAK-397 staining in BAPN treated tumors (Figure 3D, Supplemental Figure 5). In PyMT^{mgko} tumors, the K14 cell population was highly enriched for pFAK staining, with both being localized at the tumor-stromal interface. Upon BAPN treatment this enrichment of pFAK staining in these cells was diminished. These data revealed that LOX inhibition results in a loss of the keratin 14 positive myoepithelial cell phenotype in PyMT^{mgko} tumor cells and that this loss is linked with a corresponding loss of focal adhesion formation.

Stromal Cells represent the primary source of LOX in PyMT Tumors

Tumor cells cultured under hypoxic conditioned or expressing high levels of HIF1α express higher levels of LOX than their non-hypoxic counterparts(13). Thus, the increased expression of LOX could be attributed to elevated tissue hypoxia (13, 19). However, we could not establish any consistent relationship between level or distribution of tumor hypoxia when comparing the PyMT$^{fl/fl}$ and PyMT^{mgko} tumors (Supplemental Figure 6). Alternately, in human breast carcinoma, LOX expression is also a stromally produced gene that is co-expressed along with collagen type I (3, 21). Gene expression analysis on cell lines indicates that fibroblasts consistently expressed significantly more LOX when compared with epithelial tumor cells (Figure 4A). To validate these in vitro findings in vivo, laser capture microdissection (LCM) was performed on tumor sections to isolate RNA from either epithelial or stromal regions of the tumor. Upon qPCR analysis, the stroma of PyMT^{mgko} tumors expressed approximately 10 fold more LOX than the neighboring epithelium (Figure

NIH-PA Author Manuscript

NIH-PA Author Manuscript

NIH-PA Author Manuscript

4B). In situ hybridization for LOX mRNA again showed the stromal regions of PyMT^{mgko} tumors were highly enriched for LOX mRNA compared to the epithelium (Figure 4C, Supplemental Figure 7). To verify the validity and relevance of such findings to human disease, publically available datasets of LCM epithelium and stroma from invasive ductal carcinoma (IDC) were analyzed to localize LOX expression. Indeed, matching the finding in the PyMT^{mgko} tumors, IDC tumors quantitatively showed a marked increase in LOX expression in the stroma compared to the epithelium. LOX expression also aligned with genes known to be expressed in activated myofibroblasts, connective tissue growth factor (CTGF) and α-smooth muscle actin (ACTA2) all of whose expression was increased in the stroma (Figure 4D and 4E)(22). These results indicated that in both murine PyMT tumors as well as human IDC, the stroma is an abundant source of LOX.

TGF-β from Infiltrating Myeloid Cells Can Drive Fibroblast LOX Expression

We previously reported that PyMT^{mgko} tumors are characterized by increased myeloid derived suppressor cell infiltration (MDSCs) (23). MDSCs secrete abundant quantities of TGF-ß into the tumor microenvironment(23). TGF-β is a classically defined cytokine responsible for the activation of fibroblasts to αSMA expressing myofibroblasts. Corresponding with this fibroblast activation, in other mesenchymal cell types, such as lung fibroblasts and cardio myofibroblasts, TGF-β induces LOX expression in a Smad-AP1 dependent manner (24-26). When examining *in vivo* tumor progression, we observed a regional co-localization of Gr1+ myeloid cells and αSMA expressing fibroblasts (Figure 5A). This regional distribution and co-localization of Gr1+ cells and αSMA fibroblasts was consistent with the non-uniform, linearized collagen fibers we observed at the tumor periphery by second harmonic generation imaging (Figure 5B). Consistent with regional infiltration of MDSCs inducing local collagen remodeling, we quantified a spectrum of focally stiffened extracellular matrix by atomic force microscopy indentation (Figure 5C). Supporting LOX's role in this phenotype, we observed that BAPN treatment significantly reduced this variability, normalizing collagen fiber thickness and reducing stromal stiffness. To investigate the potential role of Gr1+ MDSC derived TGF-β in driving stromal LOX expression in PyMT^{mgko} tumors, a mouse mammary fibroblast cell line was treated with conditioned media from Gr1+ cells and Gr1- cells isolated from the spleens of PyMT^{mgko} tumor bearing mice. These experiments were performed with the use of the ALK 4, ALK5, and ALK7 inhibitor SB431542 to examine the necessity for TGF-β in any observed gene expression changes (27). Upon treatment, both Gr1+ and Gr1- conditioned media were able to induce expression of αSMA, a marker of fibroblast transition to an activated state in a TGF-β dependent manner. However, only TGF-β from Gr1+ cell conditioned media was able to induce the expression of LOX (Figure 5D). Interestingly, TGF-B had no such induction of LOX expression from epithelial tumor cells (Supplemental Figure 8). These data were verified by examining LOX protein levels as well as activity in the conditioned media of mouse mammary fibroblasts treated with Gr1+ and Gr1- conditioned media (Supplemental Figure 9) implicating Gr1+ derived TGF-β as a driver of stromal LOX expression in PyMT^{mgko} tumors. Additional support for this idea comes from analysis of publically available human stromal microarray datasets, which showed that stromal expression of TGF-β1 is significantly correlated with stromal LOX expression (Figure 5E). Together, these data strongly suggest that stromally expressed TGF-β acts on fibroblasts to promote the expression and activity of LOX.

Discussion

The microenvironment is an essential component in promoting tumors towards metastasis(28). While significant effort has been placed on the cellular components of the microenvironment, such as immune cells, fibroblasts and endothelial cells, one of the most

NIH-PA Author Manuscript

NIH-PA Author Manuscript

NIH-PA Author Manuscript

interesting components is the extracellular matrix (ECM). The ECM acts a foundation upon which tumors build themselves, a scaffold for blood and lymphatic vessels, and a trigger for integrin mediate cellular changes to promote growth and migration(29). As breast cancer with abrogated TGF-β signaling have substantially worse disease free survival, we sought to address the role an altered collagen matrix played in the aggressiveness of tumors (30, 31). In PyMT^{mgko} tumors, a significant increase in collagen remodeling and LOX expression was observed. Lysyl Oxidase is increased in breast cancer and associated with poor patient prognosis/metastasis [NextBio].We observed that inhibition of LOX significantly reduced tumor metastasis through decreased tumor cell intravasation. Our data indicates that LOX is stromally derived in PyMT^{mgko} tumors, thus LOX acts as a promoter of tumor metastasis independent of the cellular source and potentially through similar mechanisms. Interestingly, it appears that stromal TGF-β signaling drives this increase in LOX expression. The evidence for TGF-β promoting LOX expression and matrix remodeling thus adds another layer of complexity to the premise of therapeutically targeting TGF-β in the context of cancer.

Various tumor characteristics have been attributed to alterations of the collagenous microenvironment in tumors. Notably, hypoxic conditions drive the expression of LOX from tumor epithelium (13). As a driver for many of the phenotypes observed in our PyMT^{mgko} tumors, hypoxia was a prospective candidate for our enhanced tumorigenesis. However, no difference in hypoxia was seen leading us to look elsewhere. Previous work from our laboratory has shown that epithelial loss of functional TGFβR2 expression results in an increased recruitment of MDSCs and that this promotes tumor progression to metastasis(23). These cells are a major source of TGF-β in tumors. We show that these immature myeloid cells localize to areas of αSMA expression in PyMT^{mgko} tumors and can promote tumor matrix remodeling through TGF-β mediated stimulation of stromal fibroblasts, specifically via induced expression of LOX. It has been previously established that lung fibroblasts, as well as cardiac myofibroblasts, can express LOX upon TGF-β stimulation (24, 25). We show that this LOX promoting source of TGF-β from fibroblasts can be tumor infiltrating immune cells. Our study suggests that the tumor epithelium can indirectly promote an aggressive microenvironment through the facilitation of interactions of various components of the tumor microenvironment.

LOX is known to promote focal adhesion formation in mammary carcinoma cells, and *in vivo* inhibition of LOX suppresses both hypoxic and non-hypoxic tumor metastasis (3). Using a different mouse model of breast cancer, we have recapitulated these findings of decreased focal adhesion formation and metastasis upon inhibition of LOX with BAPN. While it should be noted that BAPN has been reported to have effects on members of the LOX family, we did not see any appreciable changes in LOXL expression (supplemental figure 2) and while certainly not quantitative, the relative Cts for the LOXL qPCR were significantly lower than those for LOX indicating lower gross expression in our tumors. As LOX acts to crosslink extracellular collagen and elastin, the induction of these phenotypes is likely due to its ability to promote stiffness in the tumor microenvironment(3, 32). Increased matrix stiffness leads to an EMT in tumor epithelium, which led us to ask if inhibition of LOX in our spontaneous tumors resulted in decreased circulating tumor cells and metastasis through the prevention of this transition(33). While no difference in the induction of EMT was observed, most likely due to a lack of TGF-β responsiveness in tumor cells used, we did see an increase in keratin 14 expression. While previously basal breast cancer cells have been shown to secrete LOX, this was the first instance in which we see LOX activity regulating this tumor cell phenotype(13, 34). Live cell imaging of K14+ mammary epithelium has shown these cells to be highly protrusive and migratory specifically in response to a collagen matrix(35). As collagen was shown to be the main driver of this migratory phenotype, modulation of the collagen matrix could abrogate this effect. This

NIH-PA Author Manuscript

NIH-PA Author Manuscript

NIH-PA Author Manuscript

indeed turned out to be the case in that inhibition of LOX resulted in fewer K14+ cells. Linking this aggressive basal phenotype with previous findings regarding the effects of LOX on the tumor epithelium, we find that K14 cells are enriched for the formation of focal adhesions in our PyMT^{mgko} tumors. The ability to adhere and respond to the extracellular matrix is an essential step in obtaining a migratory phenotype and promoting metastasis of tumor cells. As expected, inhibition of LOX activity diminished this focal adhesion enrichment. This, potentially, links not only the epithelial phenotype of these cells with their ability to respond to matrix cues, in particular matrix crosslinking and stiffness, but also to the decrease in metastasis through diminished tumor cell intravasation.

The data presented in this study show that microenvironmental changes have significant effects on tumor progression. We show that the aggressiveness of tumor epithelium is not only dictated by the genetic programming of the tumor cell but also by the state of the extracellular matrix. By demonstrating that inhibition of LOX activity cannot only inhibit tumor cell metastasis, but also modulate the phenotypic characteristics of the tumor cells, we have further refined the conceptual framework used to think about stromally targeted therapeutics. Showing that myeloid cell infiltrates can arouse stromal activation should widen the breadth of patients considered for immune modulating treatments and also provide new readouts for the efficacy of treatment options. However, while addressing many pressing issues in the field of cancer biology, our data also raise some interesting questions. We show that extracellular matrix modifications can drive phenotypic changes in basal cells, thus it is now necessary to identify the molecular basis for this interaction. Both growth factor responsiveness as well as adhesion have been shown to regulate cellular phenotypes, therefore the ability of ECM modification to promote these signaling pathways could begin to address this phenotypic switch. It is also unclear what the specific role these basal cells play in the invasive and metastatic phenotype observed. Addressing the specific migratory and invasive capacity of these different populations of cells will aid in pushing forward our knowledge of tumor metastasis. With metastasis representing the major cause of morbidity and mortality in breast cancer patients, a thorough understanding of stromal cues present in the tumor microenvironment and reciprocal epithelial responses to these cues in the context of tumor metastasis is essential.

Supplementary Material

Refer to Web version on PubMed Central for supplementary material.

Acknowledgments

Financial Support: This work is supported by NIH grants CA085492 and CA151925 to HLM and VMW, CA102162 to HLM, CA126505 and CA138818 to VMW, Susan G Komen award PDF12230246 to IA, the T.J. Martell Foundation to HLM, and CA068485 for core laboratory support. We would like to thank the Biological Imaging Development Center at UCSF for the use 2-photon microscope image acquisition and image processing facilities. Also, we would like to thank all the members of the Moses and Weaver Labs for critical help with experimentation and general discussion.

References

1. Finak G, Bertos N, Pepin F, Sadekova S, Souleimanova M, Zhao H, et al. Stromal gene expression predicts clinical outcome in breast cancer. Nature medicine. 2008; 14:518–27.
2. Khamis ZI, Sahab ZJ, Sang QX. Active roles of tumor stroma in breast cancer metastasis. International journal of breast cancer. 2012; 2012:574025. [PubMed: 22482059]
3. Levental KR, Yu H, Kass L, Lakins JN, Egeblad M, Erler JT, et al. Matrix crosslinking forces tumor progression by enhancing integrin signaling. Cell. 2009; 139:891–906. [PubMed: 19931152]

NIH-PA Author Manuscript

NIH-PA Author Manuscript

NIH-PA Author Manuscript

4. Garamszegi N, Garamszegi SP, Shehadeh LA, Scully SP. Extracellular matrix-induced gene expression in human breast cancer cells. Molecular cancer research: MCR. 2009; 7:319–29. [PubMed: 19276183]
5. Boyd NF, Guo H, Martin LJ, Sun L, Stone J, Fishell E, et al. Mammographic density and the risk and detection of breast cancer. The New England journal of medicine. 2007; 356:227–36. [PubMed: 17229950]
6. Provenzano PP, Inman DR, Eliceiri KW, Knittel JG, Yan L, Rueden CT, et al. Collagen density promotes mammary tumor initiation and progression. BMC medicine. 2008; 6:11. [PubMed: 18442412]
7. Taylor MA, Amin JD, Kirschmann DA, Schiemann WP. Lysyl oxidase contributes to mechanotransduction-mediated regulation of transforming growth factor-beta signaling in breast cancer cells. Neoplasia. 2011; 13:406–18. [PubMed: 21532881]
8. Forrester E, Chytil A, Bierie B, Aakre M, Gorska AE, Sharif-Afshar AR, et al. Effect of conditional knockout of the type II TGF-beta receptor gene in mammary epithelia on mammary gland development and polyomavirus middle T antigen induced tumor formation and metastasis. Cancer research. 2005; 65:2296–302. [PubMed: 15781643]
9. Bierie B, Stover DG, Abel TW, Chytil A, Gorska AE, Aakre M, et al. Transforming growth factor-beta regulates mammary carcinoma cell survival and interaction with the adjacent microenvironment. Cancer research. 2008; 68:1809–19. [PubMed: 18339861]
10. Gorden DL, Fingleton B, Crawford HC, Jansen DE, Lepage M, Matrisian LM. Resident stromal cell-derived MMP-9 promotes the growth of colorectal metastases in the liver microenvironment. International journal of cancer Journal international du cancer. 2007; 121:495–500. [PubMed: 17417772]
11. Bullen A, Friedman RS, Krummel MF. Two-photon imaging of the immune system: a custom technology platform for high-speed, multicolor tissue imaging of immune responses. Current topics in microbiology and immunology. 2009; 334:1–29. [PubMed: 19521679]
12. Payne SL, Hendrix MJ, Kirschmann DA. Paradoxical roles for lysyl oxidases in cancer--a prospect. Journal of cellular biochemistry. 2007; 101:1338–54. [PubMed: 17471532]
13. Erler JT, Bennewith KL, Nicolau M, Dornhofer N, Kong C, Le QT, et al. Lysyl oxidase is essential for hypoxia-induced metastasis. Nature. 2006; 440:1222–6. [PubMed: 16642001]
14. Wilmarth KR, Froines JR. In vitro and in vivo inhibition of lysyl oxidase by aminopropionitriles. Journal of toxicology and environmental health. 1992; 37:411–23. [PubMed: 1359158]
15. Bondareva A, Downey CM, Ayres F, Liu W, Boyd SK, Hallgrimsson B, et al. The lysyl oxidase inhibitor, beta-aminopropionitrile, diminishes the metastatic colonization potential of circulating breast cancer cells. PloS one. 2009; 4:e5620. [PubMed: 19440335]
16. Pantel K, Brakenhoff RH. Dissecting the metastatic cascade. Nature reviews Cancer. 2004; 4:448–56.
17. Erler JT, Bennewith KL, Cox TR, Lang G, Bird D, Koong A, et al. Hypoxia-Induced Lysyl Oxidase Is a Critical Mediator of Bone Marrow Cell Recruitment to Form the Premetastatic Niche. Cancer cell. 2009; 15:35–44. [PubMed: 19111879]
18. Rakha EA, Reis-Filho JS, Ellis IO. Basal-like breast cancer: a critical review. Journal of clinical oncology: official journal of the American Society of Clinical Oncology. 2008; 26:2568–81. [PubMed: 18487574]
19. Gatza ML, Kung HN, Blackwell KL, Dewhirst MW, Marks JR, Chi JT. Analysis of tumor environmental response and oncogenic pathway activation identifies distinct basal and luminal features in HER2-related breast tumor subtypes. Breast cancer research: BCR. 2011; 13:R62. [PubMed: 21672245]
20. Cox TR, Bird D, Baker AM, Barker HE, Ho MW, Lang G, et al. LOX-Mediated Collagen Crosslinking Is Responsible for Fibrosis-Enhanced Metastasis. Cancer research. 2013; 73:1721–32. [PubMed: 23345161]
21. Peyrol S, Raccurt M, Gerard F, Gleyzal C, Grimaud JA, Sommer P. Lysyl oxidase gene expression in the stromal reaction to in situ and invasive ductal breast carcinoma. The American journal of pathology. 1997; 150:497–507. [PubMed: 9033266]

NIH-PA Author Manuscript

NIH-PA Author Manuscript

NIH-PA Author Manuscript

22. Arora PD, McCulloch CA. Dependence of collagen remodelling on alpha-smooth muscle actin expression by fibroblasts. Journal of cellular physiology. 1994; 159:161–75. [PubMed: 8138584]
23. Yang L, Huang J, Ren X, Gorska AE, Chytil A, Aakre M, et al. Abrogation of TGF beta signaling in mammary carcinomas recruits Gr-1+CD11b+ myeloid cells that promote metastasis. Cancer cell. 2008; 13:23–35. [PubMed: 18167337]
24. Boak AM, Roy R, Berk J, Taylor L, Polgar P, Goldstein RH, et al. Regulation of lysyl oxidase expression in lung fibroblasts by transforming growth factor-beta 1 and prostaglandin E2. American journal of respiratory cell and molecular biology. 1994; 11:751–5. [PubMed: 7946403]
25. Choudhary B, Zhou J, Li P, Thomas S, Kaartinen V, Sucov HM. Absence of TGFbeta signaling in embryonic vascular smooth muscle leads to reduced lysyl oxidase expression, impaired elastogenesis, and aneurysm. Genesis. 2009; 47:115–21. [PubMed: 19165826]
26. Sethi A, Mao W, Wordinger RJ, Clark AF. Transforming growth factor-beta induces extracellular matrix protein cross-linking lysyl oxidase (LOX) genes in human trabecular meshwork cells. Investigative ophthalmology & visual science. 2011; 52:5240–50. [PubMed: 21546528]
27. Inman GJ, Nicolas FJ, Callahan JF, Harling JD, Gaster LM, Reith AD, et al. SB-431542 is a potent and specific inhibitor of transforming growth factor-beta superfamily type I activin receptor-like kinase (ALK) receptors ALK4, ALK5, and ALK7. Molecular pharmacology. 2002; 62:65–74. [PubMed: 12065756]
28. Hanahan D, Coussens LM. Accessories to the crime: functions of cells recruited to the tumor microenvironment. Cancer cell. 2012; 21:309–22. [PubMed: 22439926]
29. Lu P, Weaver VM, Werb Z. The extracellular matrix: a dynamic niche in cancer progression. The Journal of cell biology. 2012; 196:395–406. [PubMed: 22351925]
30. Bierie B, Chung CH, Parker JS, Stover DG, Cheng N, Chytil A, et al. Abrogation of TGF-beta signaling enhances chemokine production and correlates with prognosis in human breast cancer. The Journal of clinical investigation. 2009; 119:1571–82. [PubMed: 19451693]
31. Paiva CE, Serrano SV, Paiva BS, Scapulatempo-Neto C, Soares FA, Rogatto SR, et al. Absence of TGF-betaRII predicts bone and lung metastasis and is associated with poor prognosis in stage III breast tumors. Cancer biomarkers: section A of Disease markers. 2012; 11:209–17.
32. Baker AM, Bird D, Lang G, Cox TR, Erler JT. Lysyl oxidase enzymatic function increases stiffness to drive colorectal cancer progression through FAK. Oncogene. 2012
33. Leight JL, Wozniak MA, Chen S, Lynch ML, Chen CS. Matrix rigidity regulates a switch between TGF-beta1-induced apoptosis and epithelial-mesenchymal transition. Molecular biology of the cell. 2012; 23:781–91. [PubMed: 22238361]
34. Chu IM, Michalowski AM, Hoenerhoff M, Szauter KM, Luger D, Sato M, et al. GATA3 inhibits lysyl oxidase-mediated metastases of human basal triple-negative breast cancer cells. Oncogene. 2012; 31:2017–27. [PubMed: 21892208]
35. Nguyen-Ngoc KV, Cheung KJ, Brenot A, Shamir ER, Gray RS, Hines WC, et al. ECM microenvironment regulates collective migration and local dissemination in normal and malignant mammary epithelium. Proceedings of the National Academy of Sciences of the United States of America. 2012; 109:E2595–604. [PubMed: 22923691]

NIH-PA Author Manuscript
NIH-PA Author Manuscript
NIH-PA Author Manuscript

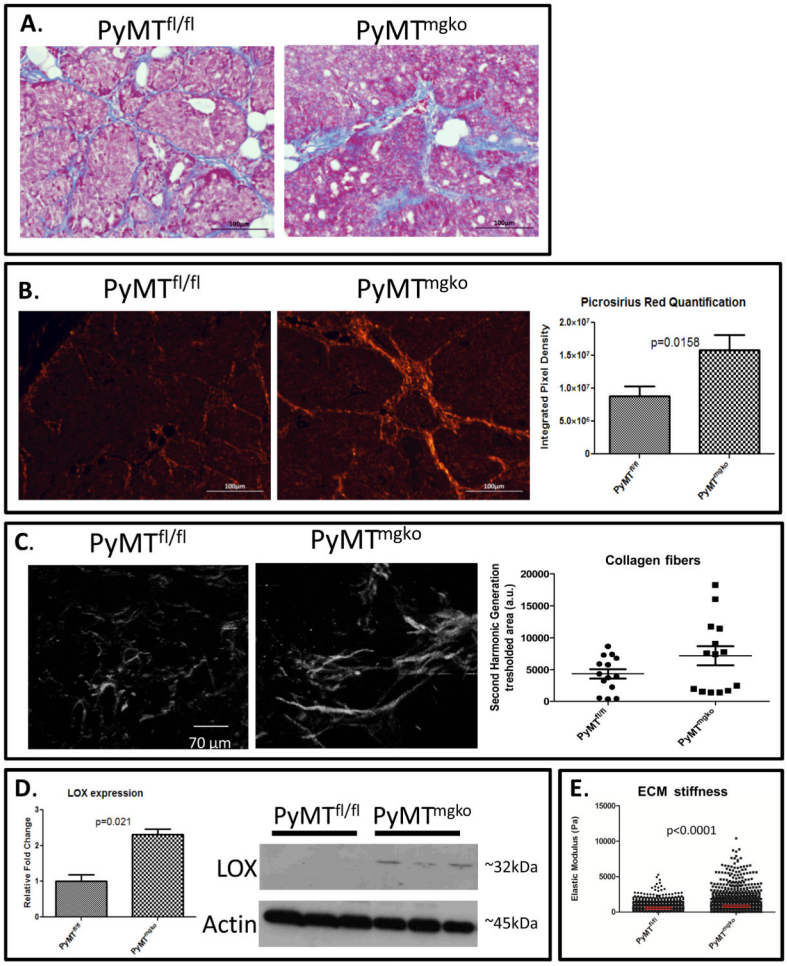

Figure 1.

Increased Collagen Deposition and LOX Expression in PyMT^{mgko} Tumors. (A) Representative images (20×) of Trichrome Blue staining of PyMT$^{fl/fl}$ and PyMT^{mgko} tumor sections. (B) Representative images (20×) of Picrosirius Red staining of PyMT$^{fl/fl}$ and PyMT^{mgko} tumor sections. Quantification of thresholded pixel density representing positive picrosirius staining for PyMT$^{fl/fl}$ ($8.8*10^6 \pm 1.4*10^6$, n=16) and PyMT^{mgko} ($2.1*10^7 \pm 2.3*10^6$, n=16) tumors. (C) Second harmonic generation (SHG) for label free imaging of fibrillar collagen. Scatter plot of SHG signal indicate a 30% increase of SHG signal in PyMT^{mgko} (7140±5696, a.u.,n=5) compared to PyMT$^{fl/fl}$ (4314±2753, a.u.,n=5) (P=0.1753 ns). (D) qPCR and western blot analysis of LOX expression in PyMT$^{fl/fl}$ (1±0.19, n=8) and PyMT^{mgko} (2.32±0.14, n=8) using whole tumor RNA and protein extracts. (E) Scatter plot of Young's Elastic Modulus of PyMT$^{fl/fl}$ and PyMT^{mgko} showing an increase of the elastic modulus of PyMT^{mgfl} stromal mammary glands (840 ± 21.61 Pa) compared to PyMT$^{fl/fl}$ (550 ± 10.54 Pa).

NIH-PA Author Manuscript
NIH-PA Author Manuscript
NIH-PA Author Manuscript

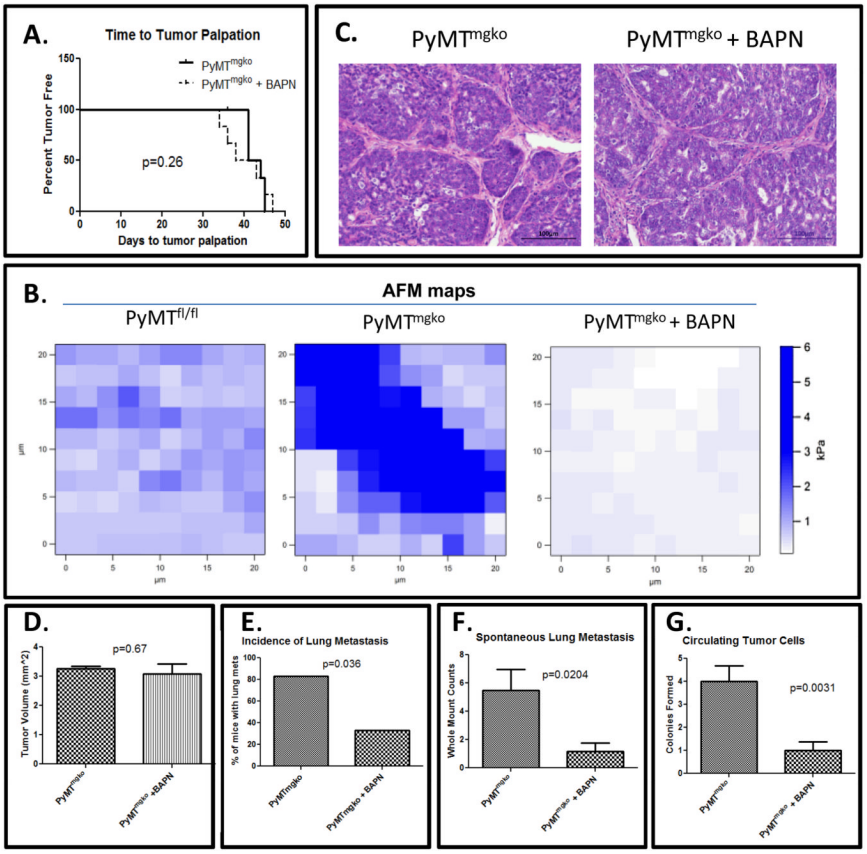

Figure 2.

LOX Inhibition Prevents Tumor Cell Metastasis Through Decreased Tumor Cell Extravasation. (A) Survival curves from birth to first palpable tumor in PyMT^{mgko} (n=8 per group) mice with and without BAPN treatment. (B) Representative AFM force maps of PyMT$^{fl/fl}$, PyMT^{mgko} and PyMT^{mgko} + BAPN stromal areas, indicating stiffer collagen in PyMT^{mgko}. BAPN treatment significantly decreased of the elastic modulus by 69.52% compared to PyMT^{mgko} (P<0.0001). (C) Representative images (20×) of Hemotoxylin and Eosin staining PyMT^{mgko} tumors treated with and without BAPN. (D) Tumor volume at the time of sacrifice in PyMT^{mgko} mice control (3.26±0.07, n=8) and BAPN treatment (3.07±0.36, n=8). (E) Incidence of tumor metastasis PyMT^{mgko} mice treated with and without BAPN presented as a percentage of the total group. (F) Quantification of the number of lung metastases per control (5.5±1.45, n=8) and BAPN treated group (1.17±0.6, n=8)(G) Quantification of the number of circulating tumor cells cultured from the circulating blood of PyMT$^{fl/fl}$ and PyMT^{mgko} mice treated with (1±0.37, n=8) and without BAPN (4±0.68, n=8). Values represent the average number of 100μm or greater colonies formed for each experimental group.

NIH-PA Author Manuscript
NIH-PA Author Manuscript
NIH-PA Author Manuscript

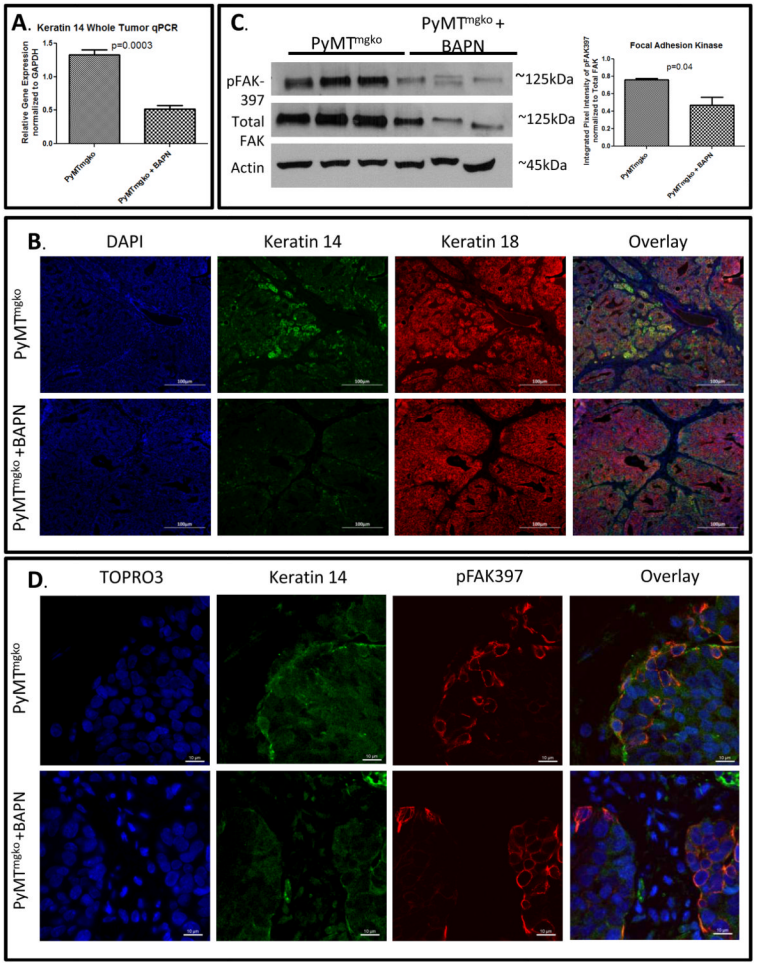

Figure 3.

LOX Activity Promotes Keratin 14 Cell Differentiation. (A) qPCR analysis of Keratin 14 expression from whole tumor RNA of PyMT^{mgko} mice with and without BAPN treatment. (B) Representative images (20×) of immunflourescent staining for Keratin 14 (Green and Keratin 18 (Red) counterstained with DAPI. Yellow seen in Overlay represents colocalization of staining. (C) Immunoblot analysis of lysates from PyMT^{mgko} and PyMT^{mgko} +BAPN tumors for phosphor-FAK(397) and Total FAK. (D) Representative images (40×) of immunoflourescent staining of phospho-FAK397 (Red) and Keratin 14 (Green) counter staining with TOPRO3.

NIH-PA Author Manuscript

NIH-PA Author Manuscript

NIH-PA Author Manuscript

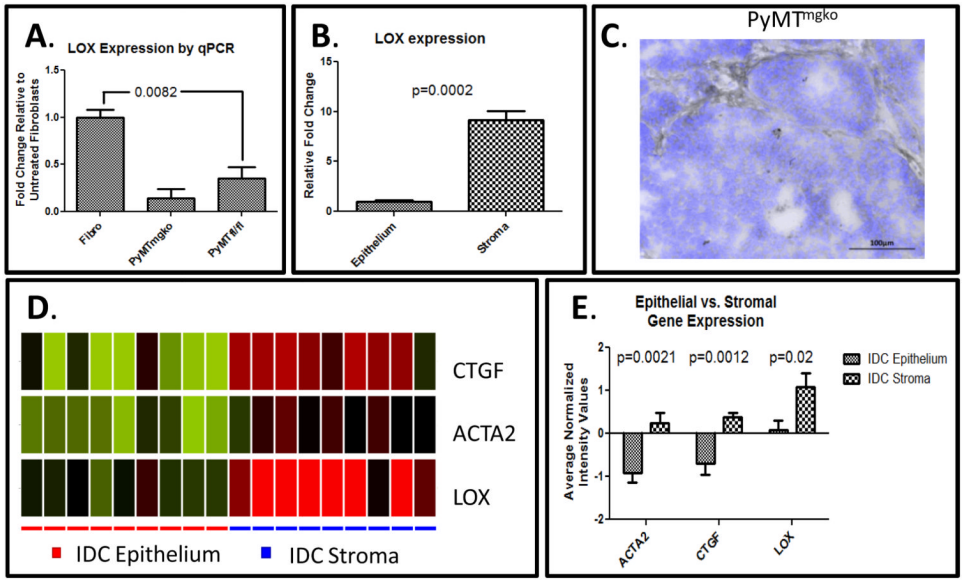

Figure 4.

Stromal Cells represent primary source of LOX in PyMT Tumors. (A) qPCR analysis of LOX expression in fibroblasts (1±0.084, n=3), PyMT^{mgko} tumor cells (0.14±0.1, n=3), and PyMT$^{fl/fl}$ tumor cells (0.3±0.12, n=3). (B) qPCR analysis for LOX from RNA extracted from epithelium (1±0.17, n=6) or stroma (9.15±0.9, n=6) from PyMT^{mgko} tumors. (C) Representative image of in situ hybridization of PyMT^{mgko} tumor counterstained with DAPI. (D) Analysis of microarray data from patient matched epithelium and stromal isolated from human invasive ductal carcinoma via LCM for ACTA2, CTGF, and LOX expression (GSE33692). Green = downregulated, Red = upregulated. (E) Quantification of normalized expression values for ACTA2, CTGF, and LOX microarray data presented in (D).

NIH-PA Author Manuscript

NIH-PA Author Manuscript

NIH-PA Author Manuscript

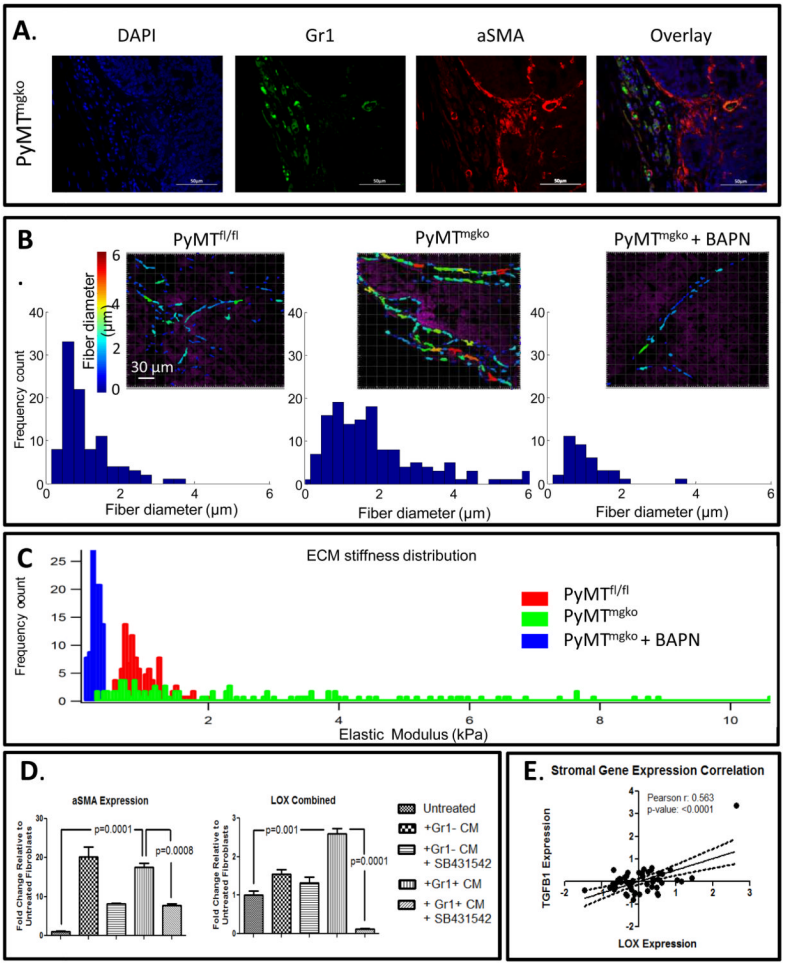

Figure 5.

TGFβ from Infiltrating Myeloid Cells Can Drive Fibroblast LOX Expression. (A) Dual Immunoflourescence localizing Gr1+ myeloid cells (Green) and aSMA expressing fibroblasts (Red) in PyMT^{mgko} tumors. (B) Top row: Representative images of ECM fibrillar collagen diameter (color-coded) and cell nuclei (purple) of PyMT$^{fl/fl}$, PyMT^{mgko} and PyMT^{mgko} + BAPN visualized with second harmonic generation (SHG) microscope. Bottom row: collagen fibers diameter quantification shows a distribution in the PyMT$^{fl/fl}$ samples with 80% of fibers with diameter falling in the range 0.4 - 2.2 μm. PyMT^{mgko} shows a wider distribution (80% of fibers with diameter falling in the range 0.6 - 3.8 μm) with respect to the PyMT$^{fl/fl}$. BAPN treatment reduced collagen accumulation and fiber thickness in PyMT^{mgko} (80% of fibers with diameter falling in the range 0.5 – 1.8 μm). (C) ECM stiffness distribution of PyMT$^{fl/fl}$ (0.1 to 2 kPa), PyMT^{mgko} (0.1 to 10 kPa) and PyMT^{mgko} + BAPN (0.1 to 0.5 kPa). (D) qPCR analysis of αSMA (also known as ACTA2) and LOX expression from fibroblasts treated with conditioned media from Gr1- or Gr1+ cells isolated from PyMT^{mgko} mice with or without SB431542 treatment. (E) Scatter plot correlating stromal TGF-ß1 expression with stromal LOX expression in human breast cancer patients (GSE9014).